Korea Australia Rheology Journal manuscript No.
(will be inserted by the editor)

Simulations of quasi-static foam flow through a diverging-converging channel

Simon Cox · I. Tudur Davies

Received: date / Accepted: date

Abstract Numerical simulations of foam flow in narrow channels are described. The fields of velocity, strain and stress are predicted for the slow flow of a dry two-dimensional foam through a diverging-converging channel. Two different bubble area dispersities are simulated, and the effects of crystallisation in the monodisperse case described.

Keywords Foams · Rheology · Surface Evolver

1 Introduction

Aqueous foams are widely used in industrial applications such as improved oil recovery and froth flotation (Cantat et al, 2013). In both of these examples the foam flows and an understanding of foam rheology is paramount in determining and optimising its performance. Particularly in the first example, and in areas such as soil remediation (Jones et al, 2013), the foam flows through narrow, constricted and tortuous channels. This article contributes to the understanding of foam flow in such situations by simulating the flow of foam through a diverging-converging channel. Ultimately we would like to be able to predict quantities such as the pressure drop required to push the foam through a given formation and the stability of the foam during such a process.

To simplify the approach, we consider here a *dry* foam (Weaire and Hutzler, 1999), that is, one in which there is little liquid between the bubbles. The interfacial films between bubbles are considered to be area minimizing, and the bubbles are therefore space-filling polyhedra with curved faces when at equilibrium. Moreover, where the bubbles meet they satisfy a particular set of geometric rules, known as Plateau's laws (Plateau, 1873), for example that films always meet in threes at equal angles of 120°. To study the fundamental aspects of foam flow, we further restrict to the consideration of two-dimensional foams, such as can be made between two parallel sheets of glass (Jones et al, 2013; Dollet and Bocher, 2015). Here, at equilibrium, each film is an arc of a circle, meeting in the afore-mentioned threes.

In order to flow, the bubbles must move past one another. They do so in a series of what are known as T1 events (Weaire and Rivier, 1984), neighbour-switching changes in which a film shrinks to zero length and is replaced by a new film approximately perpendicular to the original one. Any numerical simulation must somehow capture these events, since they contribute strongly to the mechanism by which a foam reduces its stress.

We choose to simulate foam rheology to high accuracy using the Surface Evolver (Brakke, 1992). Thus we neglect dynamic effects, such as the viscous relaxation after a T1, and assume that the foam moves slowly through a series of equilibrium states. Such an approach has previously been shown to give excellent agreement with experimental data in 2D (Jones and Cox, 2012), but is clearly highly idealized. It neglects, for example, any effects of surface tension variations due to surfactant motion and the rupture of films which is apparent in real foams. Nonetheless, as the experiments cited above demonstrate, stable, slow-flowing foams are realizable, and benchmark simulations such as those described here are an important step in understanding foam flow.

S.J. Cox
Department of Mathematics, Aberystwyth University, Aberystwyth SY23 3BZ, UK E-mail: foams@aber.ac.uk

I.T. Davies
Department of Mathematics, Aberystwyth University, Aberystwyth SY23 3BZ, UK and Coleg Cymraeg Cenedlaethol

Rossen (1990) developed a model for the pressure drop required to push foams through fractured rock by considering a single foam film in a bi-conical pore. Such a model turned out to be unexpectedly rich, with various instabilities occurring as the different geometrical parameters describing the channel are altered (Ferguson and Cox, 2013). We use that same geometry here, now with many bubbles. It mirrors recent experimental work (Dollet and Bocher, 2015) in which a foam is made to flow through a diverging channel and the deformation of the foam recorded.

We first describe our numerical method (Sect. 2) before providing extensive results on the fields of velocity, strain, plasticity, and stress in Sect. 3. Concluding remarks are made in Sect. 4.

2 Numerical Method

The Surface Evolver software (Brakke, 1992) is expressly designed for the modeling of soap bubbles, foams, and other liquid surfaces shaped by minimizing energy (such as surface tension), and subject to various constraints (such as bubble volumes). The complicated topologies found in foams are routinely handled and in particular, the Evolver can deal with the topological changes encountered during quasi-static flow. The Surface Evolver is freely available and is regularly updated.

We use the Surface Evolver to perform a quasi-static two-dimensional simulation of a disordered dry foam flowing through the channel. The input to the simulation is a list of vertices at which films (edges) meet, and ordered lists of films defining the boundary of each bubble. The walls of the channel are defined as piecewise functions of position, and certain vertices are constrained to move along the walls.

The geometric parameters of the channel are shown in Fig. 1. The channel is symmetric in both the horizontal and vertical directions, with length $2L$ and angle θ; the entrance to the channel has width $2R_b$ and entrance, exit and mid-section are rounded, to eliminate pinning of soap films, over a distance ϵ with radius of curvature $r = \epsilon/\sin\theta$. This ensures that the piecewise function describing the channel geometry is smooth, which is important for our gradient descent method.

We employ periodic boundary conditions, so that bubbles leaving the channel on the right immediately re-enter on the left. Hence, we note that the simulation could equally well be viewed as foam flow through a constriction with rapidly converging-diverging shape. For the simulation results described here, we take $L = 1$, $\theta = 42°$, $R_b = 0.2$ and $\epsilon = 0.01$.

The foam is created from a Voronoi diagram based on randomly distributed seedpoints (Brakke, 1986), and

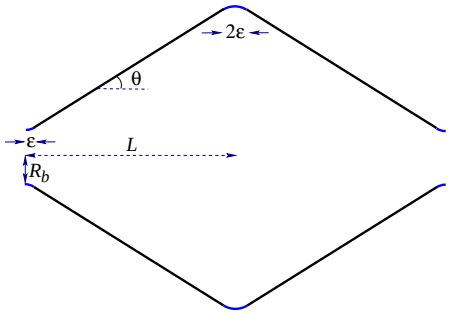

Fig. 1 Sketch of the channel shape, showing the geometric parameters used.

target bubble areas specified within Surface Evolver. To create a monodisperse foam we set all target areas to be equal, by dividing the channel area by the number of bubbles. To create a polydiserse foam, we use the areas A given by the Voronoi construction and reduce the polydispersity slightly to avoid extremely small bubbles; the value of the normalized second moment of the area distribution, $\mu_2(A) = \overline{(A/\bar{A} - 1)^2}$, is 0.275. Examples of the two foams used are shown in Fig. 2.

Since the pressure difference across each film is constant, the Young-Laplace law implies that each film can be represented as a circular arc. We chose a cut-off length $l_c = 0.0015$ for the neighbour-switching topological changes; this value is appropriate to simulate the effect of a liquid fraction of 10^{-4} (Raufaste et al, 2007), i.e. a very dry foam.

On the walls, a free slip boundary condition is imposed, recognising that a wetting film would cover the walls in an experiment and allow the Plateau borders touching the walls to move. That is, the end of a soap film touching a wall is free to move so as to make a 90° angle there (while respecting the area constraint on the adjacent bubbles). This movement is part of the gradient descent algorithm in Surface Evolver. To increase the speed of convergence, we replace any bubble films that lie along the walls with a "content integral" (Brakke and Sullivan, 1997) that represents the enclosed area; in this way we are able to use second derivative information (Hessian) during the minimization.

Foams of $N = 725$ bubbles were simulated for 1000 iterations, which takes up to 2 weeks on a desktop PC. Each iteration consists of choosing a line of films that span the channel close to the entrance to the channel and moving them downstream a small distance (Raufaste et al, 2007), before finding a minimum of surface energy (total perimeter). In this way the foam proceeds through a sequence of equilibrium states, appropriate to a situation where the foam moves very slowly and viscous effects may be neglected.

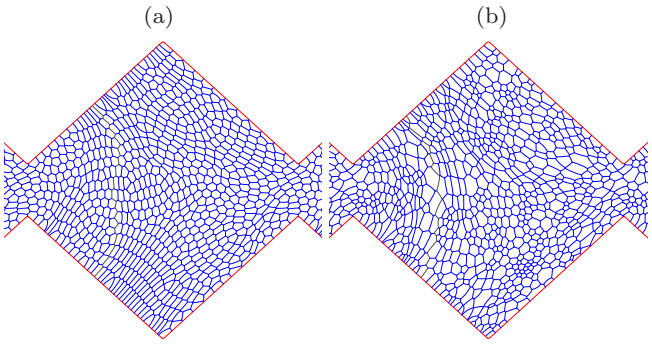

Fig. 2 Foam structures used in the simulations, shown after 1000 iterations. (a) Monodisperse. (b) Polydisperse with polydispersity $\mu_2(A) = 0.275$. Note that because the effective liquid fraction is so low, there appear to be four-fold vertices, but this is just an artefact.

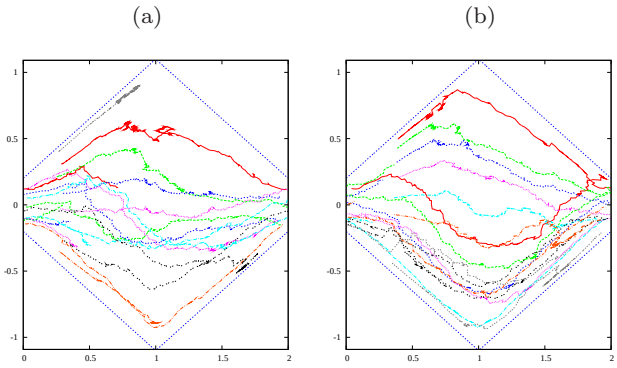

Fig. 3 Bubble paths, from left to right. (a) Monodisperse foam. (b) Polydisperse foam. Note the detachment of bubbles from the walls as the channel diverges.

3 Results

We compare the fields of velocity, texture, plasticity and stress to ascertain the effects of polydispersity on the rheology of foams in such constricted channels.

3.1 Velocity

Each bubble has a rather well-defined centre, taken as the average of its vertex positions (with care being taken to account for the periodic boundary conditions). Thus we can track the progress of each bubble through the channel. Fig. 3 shows the paths of eight bubbles, starting from a position close to the inlet of the channel, over the duration of each simulation. The length of each path gives an idea of how rapidly each bubble moves, on average. So, for example, for the monodisperse foam there is a very short track close to the upper apex of the channel, indicating that bubbles there moved very little over the whole simulation. Conversely, in the polydisperse case there was a significant amount of movement through the lower half of the channel, suggesting a preferential flow through this region. Sudden changes in direction of the path are an indicator of the occurrence of a topological change. Of particular interest are the examples of detachment of bubbles from the wall, visible in the upper left of both simulations. We attribute the higher rate of detachment in the monodisperse simulation to crystallisation (see Sect. 3.3 below).

The motion of bubble centres can also be used to generate averages of the displacement between iterations, i.e. the bubble velocity. We first average over short time intervals to detect whether or not there is a strong transient. Fig. 4 shows the horizontal velocity along perpendicular lines through the centre of the channel. The velocity along the centreline shows relatively small fluctuations about the expected U-shaped profile, with slightly greater velocities just beyond the centre of the channel in the monodisperse case. The fluctuations along the vertical line, where the velocity is lowest, are greater, indicating the strong effect of topological changes near the walls at the top and bottom of the channel. There are even regions of reverse flow far from the centreline of the channel.

Fig. 4 emphasizes the set of data from the first 100 iterations, which is relatively smooth and suggests an elastic response in both cases and along both lines. In the following, we therefore remove the first 200 iterations from the averages for velocity, strain, and stress, and the first 500 iterations for topological changes.

We assume that the flow is steady and average the displacement data over the last 800 iterations on a lattice of dimension 30×30 to give the average velocity as a function of position, as shown in Fig. 5.

As expected, the speeds are greatest in the most constricted part of the channel. The region of low speed near the apex of the channel in the monodisperse case is visible in Fig. 5(c), but otherwise the data for the two simulations are broadly similar. There is some scatter in the velocity vectors in the centre of the channel, indicating frequent changes in direction of the bubbles. However, it is apparent that velocity is not a good way to distinguish the response of foams of different polydispersity.

3.2 Strain

As bubbles pass through the channel, they are clearly deformed (Fig. 2), and capturing this deformation will give a local measure of the strain field in the foam. Highly stretched films are more likely to rupture, due to a lower concentration of surfactant, and thus strain may be a useful proxy for predicting foam break-down.

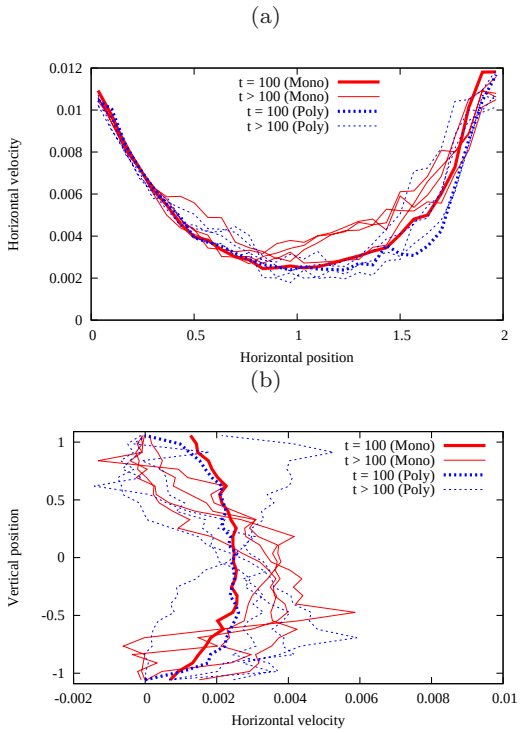

Fig. 4 The horizontal component of bubble velocity along (a) the centreline and (b) a vertical line half-way along the channel. The data is averaged over 100 iterations, and the data shown after 100, 300, ..., 900 iterations. The data for the first 100 iterations is shown as a thicker line.

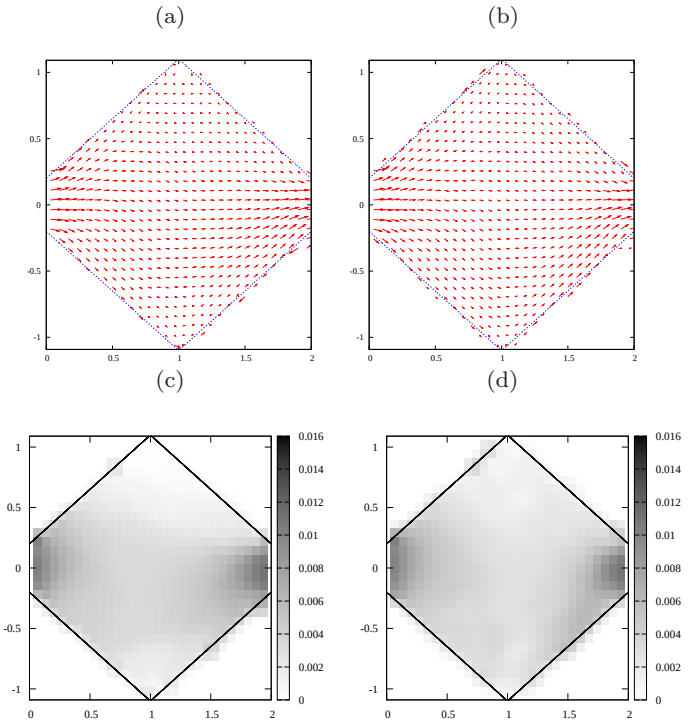

Fig. 5 Bubble velocity, averaged over 800 iterations. For each simulation the data is shown as vectors, indicating direction, in (a) and (b), and with grey value, indicating average speed, in (c) and (d). (a) and (c) Monodisperse foam. (b) and (d) Polydisperse foam.

A possible measure of strain is bubble elongation, but instead we prefer to use a tensor measure which also captures the direction in which bubbles are strained. We therefore use a "texture tensor" (Asipauskas et al, 2003; Marmottant et al, 2008) by calculating the centre of each bubble, as above, and analysing the average orientation and length of links between the centres of neighbouring bubbles.

To generate the data shown in Fig. 6 we assume that the flow is steady and average over 800 iterations on a lattice of dimension 30×30. For each lattice site we use the eigenvectors of the tensor to define the major and minor axes of an ellipse, with orientation determined by the first eigenvector. This shows the direction and magnitude of the *stretching* of bubbles. Upstream, the bubbles are compressed in the direction of flow and, because of the area constraint on each one, elongated in the perpendicular direction. This elongation decays slightly as the wall is approached and, although the differences are subtle, this decay is slightly more pronounced for the polydisperse foam. Downstream of the midpoint of the channel, the direction of elongation is reversed, and bubbles extend towards the exit. This transition occurs over quite a short distance in both simulations.

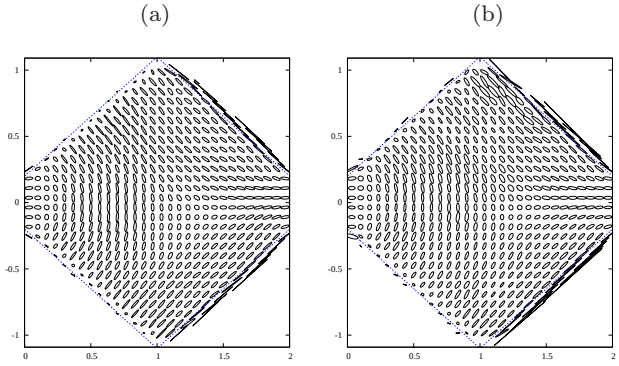

Fig. 6 Elongation information from a texture tensor, averaged over 800 iterations. (a) Monodisperse foam. (b) Polydisperse foam. Some data falls just outside the channel, due to the coarse grid on which the data is averaged, and this is ignored.

3.3 Topological changes

The topological changes, or T1s, allow bubbles to flow past each other, and hence for the foam to flow plastically. T1s are therefore a manifestation of plasticity at a mesoscopic scale. Fig. 5 indicates that there are also quiescent regions; these parts of the channel where there are no T1s correspond to elastic behaviour or plug flow.

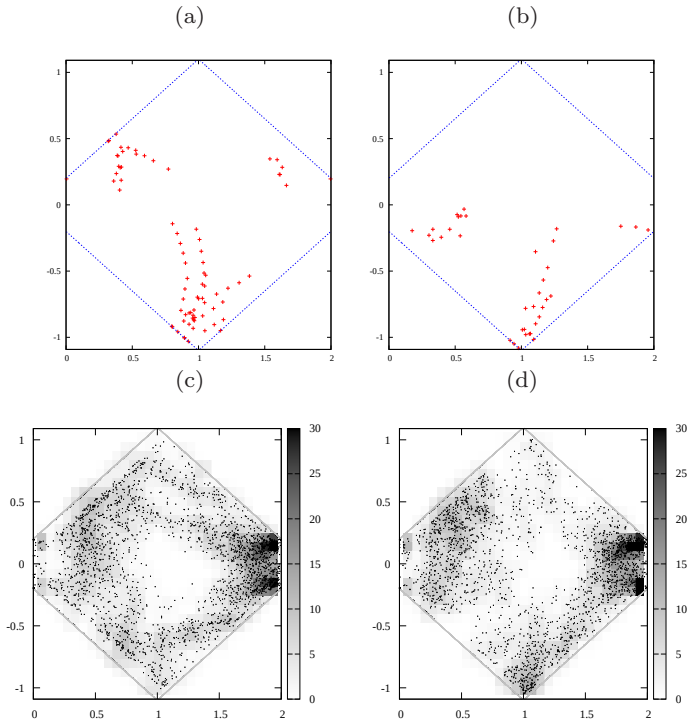

Fig. 7 The positions of topological changes. (a) All T1s during iteration 562 for the monodisperse foam. (b) All T1s during iteration 871 for the polydisperse foam. (c) All T1s during iterations 500-1000 for the monodisperse foam, shown as both individual points and by density. (c) All T1s during iterations 500-1000 for the polydisperse foam.

We record the position of each topological change at each iteration, and plot them in Fig. 7. Firstly, we choose an iteration in each simulation for which there is a relatively large number of T1s, and note that in the monodisperse foam these tend to form lines, as a result of the monodispersity. In particular, comparing with the bubble paths in Fig. 3(a), the T1s show a preference for a line across the channel from top left to the lower midpoint of the channel, mirroring the detachment of bubbles from the upper wall. The phenomenon of crystallisation in dry monodisperse foams is well-known, often leading to unrepresentative results (Durand et al, 2014). Here, it appears that a line of films forms a "weak zone" across the channel (Cox and Wyn, 2008), and this zone is maintained for much of the simulation. This behaviour is barely present in the polydisperse case.

Lines of T1s are also apparent in a plot of all T1s for the last 500 iterations, in the lower half of Fig. 7, where average T1 density is also recorded in the shading (on a 30x30 lattice). The asymmetry noted in the bubble paths (Fig. 3), with bubbles preferentially detaching from the top wall, is again apparent here, with a significant distinction between the density of T1s in the upper and lower apices of the channel. Moreover, particularly close to the diverging walls of the channel, in the monodisperse case the T1s occur in lines, reflecting the quantised distances from the wall at which films are located in a crystalline foam.

In both cases the greatest density of T1s occurs, as expected, where the bubbles approach the narrowest part of the channel. Despite the lower area of the region without T1s in the monodisperse case, i.e. the larger region of plug flow in the centre of the channel, there are 10% *more* T1s in the monodisperse simulation, and later T1s obscure earlier ones. We might therefore expect that the bubbles are less deformed in this case, but the effect is apparently not strong enough to be observed in Fig. 6.

3.4 Stress

The main contributions to the foam stress in a quasi-static simulation are from the surface tensions in the films and from the bubble pressures. Although we are able to calculate bubble pressures with high accuracy in the Surface Evolver, the average pressure is affected by our method of moving the foam by displacing a line of films and so here we present the tension contribution to the stress. This is therefore a measure of the direction in which films are oriented.

We calculate the three distinct components of the stress tensor by integrating the surface tension along each arc and summing. We assume that the flow is steady and average the data over 800 iterations on a lattice of dimension 60×60. (We use a finer lattice here compared to the velocity and texture because here we can average over films, rather than bubbles, of which there are many more.) Fig. 8 presents shear stress and extensional stress (first normal stress difference) for each simulation.

The signature of crystallization is again apparent in the monodisperse case, with alternating parallel lines of high and low stress lose to the diverging walls of the channel. The shear stress is almost (anti-)symmetric about the centreline of the channel, and greatest close to the diverging walls of the channel. Away from the walls, variations in the polydisperse case appear less well correlated. The general pattern of extensional stress is the same in both simulations, (although there is a surprising region of high variability close to the apex of the channel in the polydisperse case, breaking the symmetry about the centreline). The pale line slightly downstream from the centre of the channel, perpendicular to the direction of motion, indicates the region in which the strain re-orientates (cf. Fig. 6) as bubbles start to elongate towards the exit region.

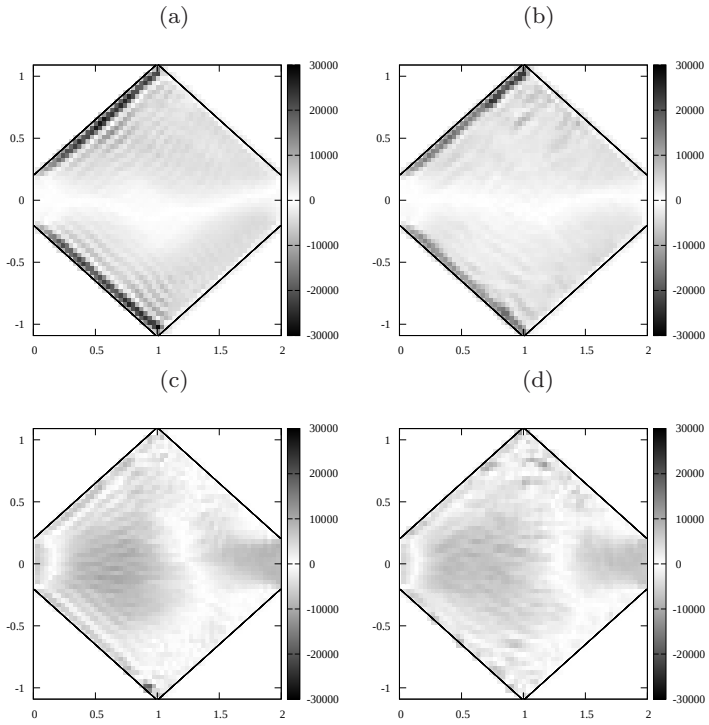

Fig. 8 Stress components averaged over 800 iterations. (a) Shear stress, monodisperse foam. (b) Shear stress, polydisperse foam. (c) Extensional stress, monodisperse foam. (d) Extensional stress, polydisperse foam.

4 Conclusion

We have performed a detailed comparison of the effects of dispersity in bubble areas in the flow of a 2D foam through a constricted channel. There are subtle yet distinct differences: for example, polydispersity suppresses any regions of static foam in the corners of the channel, the monodisperse foam is prone to localization of the velocity profile, and, again in the monodisperse case, the stress and T1 fields show strong banding parallel to the walls of the channel.

In future work, it will be of interest to vary the slope of the walls of the channel: various instabilities occur for single foam films passing through such channels (Ferguson and Cox, 2013), and we might expect to see further regions of stagnant foam as the slope increases. While it is possible to create the very dry foams simulated here, representing an extreme case of foam flow with higher stresses, more often foams contain a significant quantity of liquid, and increasing the simulated liquid fraction should lead to agreement with experiments (Dollet and Bocher, 2015). In the latter case, the bubble deformation is significantly smaller than the simulations described here, presumably because of the difference in liquid fraction. Dollet and Bocher (2015) also change the roughness of the walls in their experiments, and this inclusion of wall friction is likely something that could be achieved in simulations.

Acknowledgements We thank K. Brakke for providing the Surface Evolver. SC acknowledges funding from EPSRC (EP/N002326/1).

References

Asipauskas M, Aubouy M, Glazier J, Graner F, Jiang Y (2003) A texture tensor to quantify deformations: the example of two-dimensional flowing foams. Granular Matter **5**:71–74

Brakke K (1986) 200,000,000 Random Voronoi Polygons. www.susqu.edu/brakke/papers/voronoi.htm, Unpublished

Brakke K (1992) The Surface Evolver. Exp Math **1**:141–165

Brakke K, Sullivan J (1997) Using symmetry features of the surface evolver to study foams. In: Hege HC, Polthier K (eds) Visualization and Mathematics: Experiments, Simulations and Environments, Springer Berlin Heidelberg, pp 95–117

Cantat I, Cohen-Addad S, Elias F, Graner F, Höhler R, Pitois O, Rouyer F, Saint-Jalmes A (2013) Foams - structure and dynamics. OUP, Oxford

Cox S, Wyn A (2008) Localization of topological changes in couette and poiseuille flows of two-dimensional foams. AIP Conf Proc **1027**:836–838

Dollet B, Bocher C (2015) Flow of foam through a convergent channel. Eur Phys J E **38**:123

Durand M, Kraynik A, van Swol F, Käfer J, Quilliet C, Cox S, Talebi S, Graner F (2014) Statistical Mechanics of Two-Dimensional Shuffled Foams, part II: Geometry - Topology Correlation in Small or Large Disorder Limits. Phys Rev E **89**:062,309

Ferguson D, Cox S (2013) The motion of a foam lamella traversing an idealised bi-conical pore with a rounded central region. Coll Surf A **438**:56–62

Jones S, Cox S (2012) On the effectiveness of a quasi-static bubble-scale simulation in predicting the constriction flow of a two-dimensional foam. J Rheol **56**:457–471

Jones S, Dollet B, Meheust Y, Cox S, Cantat I (2013) Structure-dependent mobility of a dry aqueous foam flowing along two parallel channels. Phys Fluids **25**:063,101

Marmottant P, Raufaste C, Graner F (2008) Discrete rearranging disordered patterns, part II: 2D plasticity, elasticity and flow of a foam. Eur Phys J E **25**:371–384

Plateau J (1873) Statique Expérimentale et Théorique des Liquides Soumis aux Seules Forces Moléculaires. Gauthier-Villars, Paris

Raufaste C, Dollet B, Cox S, Jiang Y, Graner F (2007) Yield drag in a two-dimensional foam flow around a circular obstacle: Effect of liquid fraction. Euro Phys J E **23**:217–228

Rossen W (1990) Theory of Mobilization Pressure Gradient of Flowing Foams in Porous Media. J Coll Interf Sci **136**:1–53

Weaire D, Hutzler S (1999) The Physics of Foams. Clarendon Press, Oxford

Weaire D, Rivier N (1984) Soap, cells and statistics–random patterns in two dimensions. Contemp Phys **25**:59–99